7 Particle Physics at DESY/HERA (H1)

K. Müller, K. Nowak, P. Robmann, A. Schöning, U. Straumann, and P. Truöl

in collaboration with:
C. Grab and M. Sauter, Institut für Teilchenphysik der ETH, Zürich, S. Egli, M. Hildebrandt, and R. Horisberger, Paul Scherrer Institut, Villigen, and 37 institutes outside Switzerland

(H1 - Collaboration)

Since the end of the running period of HERA in 2007 the collaboration concentrates on the analysis of the high quality HERA-II data sets collected in the years 2004-2007 after the upgrade of the H1 detector with an integrated luminosity of 238 pb^{-1} for collisions with electrons and 219 pb^{-1} for collisions with positrons. The final months of HERA operation were devoted to collisions at lower proton energies: 6.2 pb^{-1} and 12.4 pb^{-1} were collected with 27.4 GeV positrons colliding with 575 or 460 GeV protons, respectively. This data has been used for a first direct measurement of the longitudinal structure function F_L(1).

In fifteen years of data taking, the results of the H1 and ZEUS experiments already found their way into the textbooks. Besides the deep insight into the structure of the proton at very small distances which has a major impact on the LHC experiments, the HERA measurements confirmed the nature of the strong force and showed that indeed the weak and the electromagnetic force have the same strength at high momentum transfer and can be unified into the electroweak force. The full data set of HERA allows to present most of the final results with low statistical and systematical errors.

Nine publications (1) – (9) and many contributions to the XVI International Conference on High energy Physics in Philadelphia 2009 (10) – (33) document the continuing effort in the analysis of the H1 data. New results, partly preliminary (34), which deserve to be mentioned, concern the following topics:

- Direct measurement of the longitudinal structure function F_L at medium Q^2 (1).
- Precise determination of the neutral electroweak current cross sections over a large range of the squared four momentum transfer Q^2 and the extraction of the parton density functions (PDF) (11; 12).
- Multi-jets at high and low Q^2 leading to an improved determination of the running coupling constant α_s (13).
- Photo-produced diffractive dijets (14), diffractive ρ- and ϕ-mesons (16), inelastic J/ψ (15), beauty (25) and D^*-mesons (21), and prompt photons (20).
- Search for states and interactions outside the Standard Model (SM), such as leptoquarks (17), single top production, excited electrons and quarks (9; 18), multi-lepton production (8) and isolated leptons with large missing momentum (4).
- Strangeness (5; 23) and D^*-meson (28) production in deep inelastic scattering, charm fragmentation (6) and the extraction of the charm and beauty contribution to the proton structure function (29; 30).

In the past years our analysis effort concentrated on events with isolated photons produced in either photoproduction ($Q^2 \approx 0$), as discussed below (Sec. 7.3), or deep inelastic scattering ($Q^2 > 4$ GeV^2). The latter is already published (35; 36) and has been described in previous annual reports (37).

7.1 Single top production

Top quarks are of particular interest in searches for new physics because of the large top mass which is close to the electroweak scale. In ep collisions top production in the standard model is strongly suppressed, hence the observation of single top production would be a clear indication of a new physics process. Several extensions of the SM predict the top quark to undergo flavour changing neutral current interactions (FCNC) which could lead to a sizeable cross section at HERA ($ep \to \nu t b X$).

A search for single top production was performed using the full $e^{\pm}p$ data set with a total integrated luminosity of 474 pb^{-1}. Single top production is detected via the decay of the top quark $t \to bW$.In the case of leptonic decays of the W the signature is a charged lepton and missing transverse momentum, accompanied by a high transverse momentum (P_T) hadronic final state from the fragmentation of the b quark. The signature for single top production with a subsequent hadronic decay of the W is three high P_T jets with an invariant mass compatible with the top mass. To estimate a possible top quark contribution in a sample with isolated leptons or high P_T jets, a top quark candidate is reconstructed from its decay products (lepton or two jets, neutrinos and b quark). Three observables are defined to discriminate the top signal from QCD background corresponding to the transverse momentum of the reconstructed b quark, the invariant mass of the reconstructed top and the W decay angle.

A multivariate discriminant based on a neural network is formed to differentiate top quark candidates from SM background. Fig. 7.1 shows the discriminator D for the electron and the muon channel. The SM background, mainly from W production is located at small values of D whereas the expectation for a single top signal is at large values of D. Also shown are the data events as classified by the discriminator. The observed slight excess of events with an isolated lepton and high missing transverse momentum has already been reported in previous years(4; 38; 39). The signal cross section is extracted from the discriminator spectra using the fractional event counting which takes statistical and systematical uncertainties into account. For all channels combined an upper bound of the cross section for anomalous single top production via FCNC is:

$$\sigma(ep \to etX) < 0.25 \text{ pb} .$$

The limits on the cross section are converted to limits at 95% CL on the anomalous FCNC coupling $\kappa_{tu\gamma}$. They are shown in Fig. 7.2 with

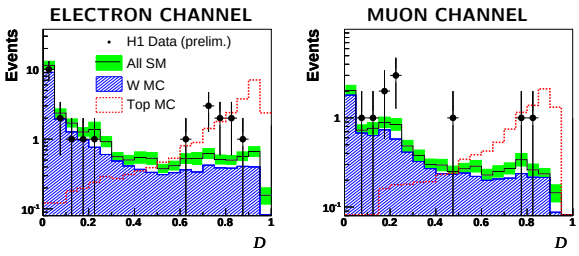

Figure 7.1: Distribution of the discriminant which is used to differentiate single top production from SM background processes for the channel with an isolated electron (left) and an isolated muon (right).

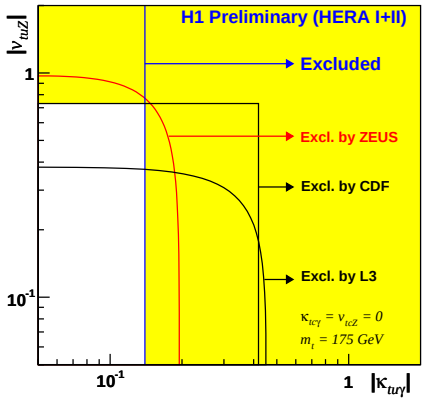

Figure 7.2: Exclusion limit at 95% CL on the anomolous $\kappa_{tc\gamma}$ and v_{tuZ} couplings. The domain excluded by H1 is represented by the light shaded area.

the limits of other experiments. The limit of the ZEUS (40) experiment which is based on HERA1 data only are only slightly weaker, mainly reflecting the top like events observed by H1 and not by ZEUS. The measurement has been presented to several conferences and is in the process of being published.

7.2 Measurement of $F_2^{c\bar{c}}$ and $F_2^{b\bar{b}}$

The measurement of inclusive charm (c) and beauty (b) quark cross sections in deep inelastic scattering at HERA provides an important test of QCD. The charm structure function $F_2^{c\bar{c}}$ and the beauty structure function $F_2^{b\bar{b}}$ are obtained from a measurement of the cross section of events containing heavy quarks. They are distinguished from events containing light quarks using variables reconstructed in the H1 Silicon Vertex Detector. The most important of these variables is the significance, defined as the transverse displacement of tracks from the primary vertex divided by the error. For events with three or more tracks in the vertex detector the reconstructed variables are used as input to a neural net. The fractions of c, b and light quarks are extracted in each bin by a least square simultaneous fit to the NN output and the significance of the two tracks with the highest significance.

The fraction of the beauty cross section to the total cross section varies from 0.2% at $Q^2 = 5$ GeV^2 to 1.0% at $Q^2 = 60$ GeV^2. The fraction of the charm cross section is 16% in average and increases slightly with increasing Q^2 and decreasing x. The measurement of $F_2^{c\bar{c}}$ as a function of Q^2 is shown in Fig. 7.3. The data are compared to a NLO (41) and a NNLO(42) calculation, which gives a better description at low Bjorken x, the momentum fraction carried by the struck quark. The measurement has been presented on various conferences (29) and will soon be published.

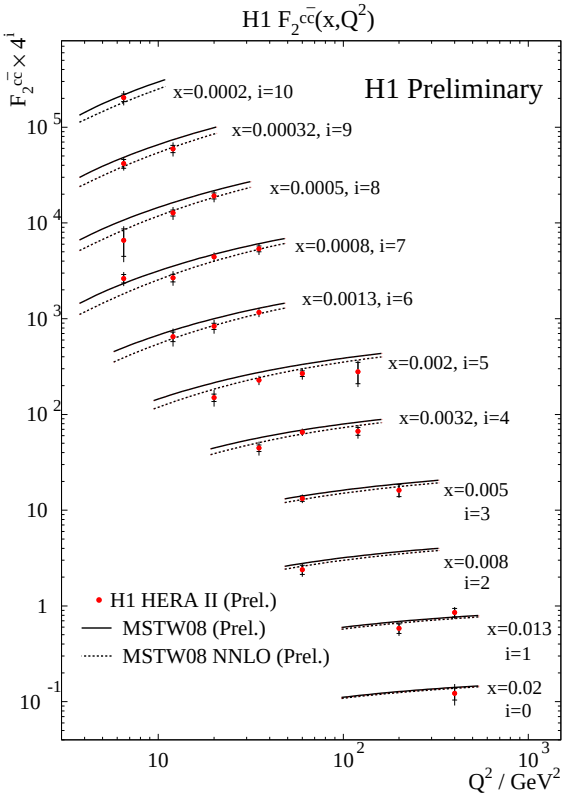

Figure 7.3: The charm structure function $F_2^{c\bar{c}}$ as a function of Q^2 for various x values. The inner error bars show the statistical error, the outer error bars represent the statistical and systematic errors in quadrature. QCD predictions at NLO are shown as dotted line and at NNLO as full line.

7.3 Isolated photons in photoproduction

Events with an isolated photon emerging from the hard subprocess $ep \rightarrow e\gamma X$ - so called prompt photons - are a powerful probe of the dynamics of the hard subprocess. They require generally lower corrections for hadronisation than measurements relying on jets, since the photons emerge without the hadronisation process by which final state quarks or gluons form a jet. Production of isolated photons with high transverse momentum can be calculated in QCD, but previous measurements have shown that higher order cor-

rections are important. In photoproduction (PhD thesis of Krzysztof Nowak) at very low Q^2 the scattered electron escapes detection through the beam pipe. The exchanged quasi-real photon either interacts directly with a parton from the proton (direct contribution) or resolves into partons which take part in the interaction (resolved contribution). Hence, the cross section yields information on the quark and gluon densities in the photon and the proton with different and generally lower corrections for hadronisation than in jet measurements. The data collected during 2004-2007 correspond to a total integrated luminosity of 340 pb^{-1}, three times the value of the previous measurement.

Isolated photons with transverse energy $6 < E_T^\gamma < 15$ GeV and pseudorapidity $-1.0 < \eta^\gamma < 2.4$ are selected in events with inelasticity $0.1 < y < 0.7$. This considerably extends the phase space of previous measurements at HERA towards larger pseudorapidities of the photon and to lower event inelasticities. To ensure isolation of the photon, the energy fraction z of the photon-jet carried by the photon candidate has to to be larger than 90% ($z \equiv E^\gamma / E^{photon-jet} > 0.9$). The isolation rejects a large part from the background from decay photons of neutral hadrons in dijet photoproduction events. The photon signal is extracted by combining different shower shape variables into a discriminator and then unfolding the photon signal. A regularised unfolding procedure (43) is used to relate the measured observables to the true variables on hadron level, determine the fraction of signal and background and to correct the data for the detector acceptance. The observables are the transverse energy E_T^γ and pseudorapidity η^γ of the photon. Each E_T^γ-η^γ bin is further divided into bins in variables depending on jet properties for the exclusive measurements. In addition, each measurement bin is binned in the discriminator D to allow the discrimination of signal and background. The unfolding matrix is computed using the PYTHIA(44) simulations for the signal and the background.

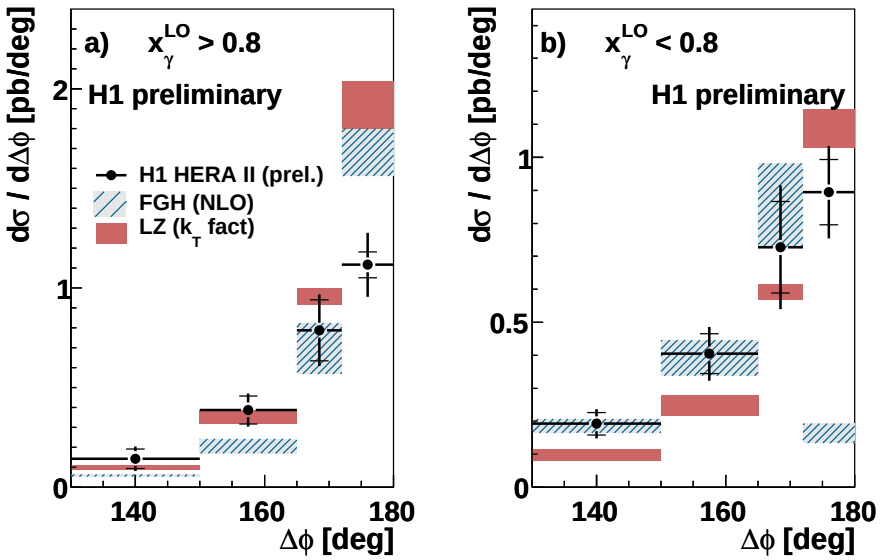

Figure 7.4: Differential prompt photon plus jet cross sections $d\sigma/d\Delta\Phi$ for a sample with the direct (a) and the resolved (b) contribution enhanced. The cross section is measured for photons with transverse energy $6 < E_T^\gamma < 15$ GeV and pseudorapidity $-1.0 < \eta^\gamma < 2.43$ accompanied by a hadronic jet with $E_T^{jet} > 4.5$ GeV and $-1.3 < \eta^{jet} < 2.3$. The inelasticity is restricted to $0.1 < y < 0.7$.

Transverse correlations between the photon and the jet are studied for prompt photons accompanied by a hadronic jet. They are particularly sensitive to higher order gluon emission. Fig. 7.4 shows the azimuthal acoplanarity between the photon and the jetfor (a) $x_\gamma^{LO} > 0.8$ where the direct interaction of a photon with the proton dominates and for (b) $x_\gamma^{LO} < 0.8$ with a significant contribution of events with a resolved photon. The data are compared to a NLO calculation (45), denoted by FGH, and a calculation based on the k_T factorisation approach which uses the un-integrated quark and gluon densities of the proton and the photon according to the Kimber-Martin-Ryskin prescription (46) (LZ).

Both predictions slightly overestimate the back-to-back configuration for $x_\gamma^{LO} > 0.8$. For $x_\gamma^{LO} < 0.8$ there is a lower contribution from the back-to-back configuration and the photon tends to be closer to the jet. This reflects the increased contributions from events with a resolved photon and from photons radiated from quarks. FGH describes the distributions within the errors, except for the highest bin in $\Delta\Phi$ for $x_\gamma^{LO} < 0.8$. This region is sensitive to multiple soft gluon radiation which limits the validity of fixed order calculations. The LZ predicts a significantly lower contribution of events with no back-to-back signature.

[1] F. D. Aaron *et al.* [H1 Collaboration], Phys. Lett. B **665** (2008) 139, arXiv:0805.2809 [hep-ex].

[2] **A General Search for New Phenomena at HERA**, F. D. Aaron *et al.* [H1 Collaboration], arXiv:0901.0507 [hep-ex].

[3] F. D. Aaron *et al.* [H1 Collaboration], Phys. Lett. B **673** (2009) 119, arXiv:0901.0477 [hep-ex].

[4] **Events with Isolated Leptons and Missing Transverse Momentum and Measurement of W Production at HERA**, F. D. Aaron *et al.* [H1 Collaboration], arXiv:0901.0488 [hep-ex].

[5] **Strangeness Production at low Q^2 in Deep-Inelastic ep Scattering at HERA**, F. D. Aaron *et al.* [H1 Collaboration],

[6] F. D. Aaron *et al.* [H1 Collaboration], Eur. Phys. J. C **59** (2009) 589, arXiv:0808.1003 [hep-ex].

[7] F. D. Aaron *et al.* [H1 Collaboration], Phys. Lett. B **672** (2009) 219, arXiv:0810.3096 [hep-ex].

[8] F. D. Aaron *et al.* [H1 Collaboration], Phys. Lett. B **668** (2008) 268, arXiv:0806.3987 [hep-ex].

[9] F. D. Aaron *et al.* [H1 Collaboration], Phys. Lett. B **666** (2008) 131, arXiv:0805.4530 [hep-ex].

[10] Contributed papers by the H1-Coll. to ICHEP2008, 34th International Conference on High Energy Physics, Philadelphia, USA, 30/7 - 5/8 2008; papers are listed, which are not yet submitted to journals.

[11] **HERA I PDF Fit: Extraction of the proton parton density functions using a NLO-QCD fit of the combined H1 and ZEUS inclusive DIS cross sections** [10].

[12] **High Q^2 NC analysis using the complete HERA data** [10].

[13] **Inclusive and Multi-Jet Production at high Q^2 and determination of α_s using full HERA data** [10].

[14] **Diffractive photoproduction of jets with the H1 detector** [10].

[15] **Inelastic Photo-Production of J/Psi Mesons at HERA** [10].

[16] **Diffractive rho and phi production in DIS with the H1 detector** [10].

[17] **A search for Leptoquarks in ep collisions at HERA** [10].

[18] **A search for excited quarks in ep collisions at HERA** [10].

[19] **Multiparton interactions in photoproduction of dijets at H1** [10].

[20] **Prompt photons in photoproduction at HERA II** [10].

[21] **Measurement of the D^* production cross section in photoproduction with the H1 detector using HERA II data** [10].

[22] **Measurement of jet production in deep-inelatic ep scattering at low Q^2** [10].

[23] **Strangeness Production at low Q^2 in Deep-inelastic ep Scattering at HERA** [10].

[24] **Measurement of the Inclusive ep Scattering Cross Section at medium Q^2 and x at HERA** [10].

[25] **A Measurement of Beauty Photoproduction Through Decays to Muons at HERA-II** [10].

[26] **Charm Production at large Q^2 in deep inelastic electron-proton scattering at HERA** [10].

[27] **The Charm Fragmentation Function in DIS** [10].

[28] **D^* production at medium/low Q^2 with the H1 detector** [10].

[29] **Measurement of F_2^{cc} and F_2^{bb} using the H1 vertex detector at HERA** [10].

[30] **Extraction of the Charm Contribution to the Proton Structure Function F_2^C from $D^{*\pm}$ Measurements in Deep Inelastic Scattering at HERA** [10].

[31] **Leading Neutron production in DIS at HERA** [10].

[32] **Inclusive $K^{*\pm}$ production at low Q^2 at HERA** [10].

[33] **Search for a $D*$p resonance at HERA II** [10].

[34] Preliminary H1 results to be presented at the 2009 Workshop on Deep Inelastic Scattering (DIS 2009), Madrid, April 7-11, 2009; available at *http://www-h1.desy.de/publications/H1preliminary.short_list.html*.

[35] F. D. Aaron *et al.* [H1 Collaboration], Eur. Phys. J. C **54** (2008) 371, arXiv:0711.4578 [hep-ex].

[36] **Isolated photon production in deep-inelastic scattering at HERA**, Carsten Schmitz, PhD Thesis, University of Zürich (2007) available at http://www-h1.desy.de/publications/theses_list.html.

[37] Physik-Institut, University of Zürich, Annual Reports 1996/7 ff.; available at *http://www.physik.unizh.ch/reports.html*.

[38] V. Andreev *et al.* [H1 Collaboration], Phys. Lett. B **561** (2003) 241, arXiv:0301030 [hep-ex].

[39] C. Adloff *et al.* [H1 Collaboration], Eur. Phys. J. C **5** (1998) 575, arXiv:9806009 [hep-ex].

[40] S. Chekanov *et al.* [ZEUS Collaboration], Phys. Lett. B **559** (2003) 153, arXiv:0302010 [hep-ex].

[41] A. D. Martin, W. J. Stirling, R. S. Thorne and G. Watt, "Parton distributions for the LHC," arXiv:0901.0002 [hep-ph].

[42] R. S. Thorne, Phys. Rev. D **73** (2006) 054019, arXiv:0601245 [hep-ph].

[43] V. Blobel, "An unfolding method for high energy physics experiments," Proc. Advanced Statistical Techniques in Particle Physics, Durham (2002).

[44] T. Sjöstrand *et al.*, PYTHIA 6.2 Physics and Manual, arXiv:0108264 [hep-ph].

[45] M. Fontannaz, J. P. Guillet and G. Heinrich, Eur. Phys. J. C **21** (2001) 303.

[46] A. V. Lipatov and N. P. Zotov, Phys. Rev. D **72** (2005) 054002.